

# SPECTROSCOPIC STUDIES ON ISATIN-3-SEMICARBAZONE AND ISATIN-3-THIOSEMICARBAZONE.

N. T. AKINCHAN

(Received 14 January, 2004; Revision Accepted 9 June, 2004)

## ABSTRACT

The configurations of semi-and thiosemicarbazone derivatives of isatin are assigned by means of  $^1\text{H}$  and  $^{13}\text{C}$  NMR Spectroscopy including NOE difference spectra, IR and electronic spectral data of these compounds are also reported and discussed. The electron impact (EI), fast atom bombardment (FAB) and negative ion chemical ionization (NICI) mass spectra are also reported. Fragmentation of molecular and pseudomolecular ions are tabulated and rationalized.

**KEYWORDS:**  $^1\text{H}$  NMR,  $^{13}\text{C}$  NMR, Semicarbazone thiosemicarbazone, mass spectra, negative ion chemical ionization, fragmentation.

## INTRODUCTION

Thio-semicarbazone derivatives of isatin and N-methyl isatin represent interesting class of bioactive compounds due to their antiviral activities (Levinson, 1980, Levy et al 1976, Sherman et al, 1980, Wang and Levinson, 1978). The antiviral activities are dependent upon the thiosemicarbazide side chain since semicarbazide derivatives are inactive (Levinson, 1980). There has been considerable interest shown in the coordination chemistry of isatin-3-semicarbazone (Akinchan et al 1994, Chatterjee, et al 1989) and isatin-3-thiosemicarbazone. (Akinchan et al, 2002, Ivanov et al. 1988; Labisbal et al., 2002, Selem et al., 2002; West et al, 1998) in recent times.

The Homonuclear NOE(Nuclear Overhauser Effect) difference spectroscopy is a convenient tool for configuration assignment and it has been employed for thiosemicarbazone derivatives of aldehydes and ketones (Easmon et al, 1993; Heinisch and Holzer, 1990). NMR spectral assignments for isatin and N-acyl-isatin (Angell et al, 1992) have been reported. There is scarcity of information on NMR and mass spectral data on isatin-3-semicarbazone and isatin-3-thiosemicarbazone. The present article describes NMR and mass spectral studies on the above mentioned compounds.

## MATERIALS AND METHODS.

### Synthesis of -3-Isatin Thiosemicarbazone (ISTSCH)

Isatin and thiosemicarbazide were dissolved in aqueous ethanol in equimolar ratio and the resulting yellow solution was refluxed for one hour on a water bath. On cooling to  $25^\circ\text{C}$  a yellow crystalline product was isolated and washed with ethanol and diethylether and dried over fused  $\text{CaCl}_2$  Yield 80%. FAB<sup>+</sup> MS, m/z 221 (M + H<sup>+</sup> 100%). Anal Calcd. For  $\text{C}_9\text{H}_8\text{N}_4\text{SO}$  (220.25): C 49.08, N 25.44, H 3.66. Found C 49.16, N 25.32, H 3.60.

### Synthesis of Isatin-3-Semicarbazone (ISSCH)

Isatin, semicarbazide hydrochloride and sodium acetate were dissolved in aqueous ethanol in an equimolar ratio and the resulting yellow solution was refluxed for 30

minutes on a water bath. On cooling to  $25^\circ\text{C}$  a yellow crystalline product was isolated and washed with ethanol and diethyl ether and dried over fused  $\text{CaCl}_2$ . Yield 78%. FAB<sup>+</sup> MS, m/z 205 (M + H<sup>+</sup>, 100%). Anal. Calcd. For  $\text{C}_9\text{H}_8\text{N}_4\text{O}_2$  (204.19) C 52.94, N 27.44, H 3.95. Found C 52.78, N 27.35, H 3.98.

### Analyses

Dried samples were used for all the analyses and measurements. Carbon, hydrogen and nitrogen were determined by the standard micro method at Regional Sophisticated Instrumentation Centre, Central Drug Research Institute, Lucknow, India.

### $^1\text{H}$ NMR Spectral measurements

The NMR spectra were recorded in DMSO- $d_6$  solutions on a Bruker Am-300 on a Bruker Am-400 Fourier Transform Spectrometer equipped with an aspect 3000 computer (operating frequency 300 MHz or 400 MHz). The probe temperature were  $28^\circ\text{C}$  or ambient. The centre of the solvent multiplet was used as internal standard, which was related to TMS by 2.49 ppm. NOE difference experiments were performed with non-degassed solutions using the frequency cyclic method of Kinns and Sanders (Bruker NOE mult). Several recordings were made on varian unityplus 300 NMR spectrometer (300 MHz for  $^1\text{H}$ ) at Vienna, Austria. 8K data point, spectral width 5999 HZ, acquisition time 3.74s, irradiation time 5s, irradiation power 57 db.

### $^{13}\text{C}$ NMR Spectral measurements

$^{13}\text{C}$  NMR Spectra were recorded on the same spectrometer as described above (operating frequency, 75 MHz or 100MHz). The probe temperature was  $28^\circ\text{C}$  or ambient. The centre of the solvent multiplet was used as internal standard, which was related to TMS by 39.50ppm.  $^1\text{H}$  decoupled  $^{13}\text{C}$  NMR spectra were obtained using the gated decoupling technique. Acquisition parameters: 16K data point, spectral width. 11,373 Hz, acquisition time 3.5s. Several recordings were made on varian Unityplus 300 NMR Spectrometry (75, MHz for  $^{13}\text{C}$ ) at Vienna, Austria.

Table 1:  $^1\text{H}$  and  $^{13}\text{C}$  NMR chemical shifts ( $\delta$ , ppm) for E-ISSCH and Z-ISTSCH in  $\text{DMSO-d}_6$ 

$^{13}\text{C}$	E-ISSCH	Z-ISTSCH	$^1\text{H}$	E-ISSCH	Z-ISTSCH
C(2)	164.90(s)	162.6(s)	C(4)H	8.08(d)	7.63(d)
C(3)	133.3 (s)	132.0 (s)	C(5)H	7.00 (t)	7.05 (t)
C(3a)	115.7 (s)	119.9 (s)	C(6)H	7.32 (t)	7.32 (t)
C(4)	125.2 (d)	120.9 (d)	C(7)H	6.88 (d)	6.90 (d)
			N(1)H	10.71(s)	12.45(s)
C(5)	121.6 (d)	122.3 (d)	N-NH	10.20 (s)	11.12 (s)
C(6)	131.6 (d)	131.2 (d)			
			NH <sub>2</sub>	6.91 (s)	8.63 (s)
C(7)	110.4 (d)	111.0 (d)			9.01 (s)
C(7a)	142.9 (s)	142.3 (s)			
C = X (O,S)	156.0 (s)	178.7 (s)			

Table 2: Results of long range INEPT experiments

(E)-ISSCH		(Z)-ISTSCH	
Selected proton resonance irradiated (ppm)	Excited carbon Signals observed (ppm)	selected proton resonance irradiated (ppm)	Excited carbon signals observed (ppm)
7.00(H-5)	115.7(C-3a) 110.4(C-7)	7.05(H-5)	119.9(C-3a) 111.0(C-7)
7.32(H-6)	142.9(C-7a) 125.2(C-4)	7.32(H-6)	142.3(C-7a) 120.9(C-4)
6.88(H-7)	121.6(C-5) 115.7(C-3a)	6.90(H-7)	122.3(C-5) 119.9(C-3a)
8.08(H-4)	142.9(C-7a) 133.3(C-3) 131.6(C-6) 115.7(C-3a)	7.63(H-4)	142.3(C-7a) 132.0(C-3) 131.2(C-6)

Table 3: Selected IR spectral bands  $\text{cm}^{-1}$  of E-ISSCH and Z-ISTSCH

E-ISSCH	Z-ISTSCH	Assignments
3464	3520	$\nu_{\text{as}}(\text{NH}_2)$
3412	3424	$\nu_{\text{as}}(\text{NH}_2)$
3238	3170	$\nu_{\text{s}}(\text{NH})$ Hydrazone
3353	3337	$\nu(\text{NH})$ indole
3294	3267	
1725	1700	$\nu(\text{C}=\text{O})$ indole
1698		$\nu(\text{C}=\text{O})$ semicarbazide
1635	1675	$\delta(\text{NH}_2)$
1653	1651	$\nu(\text{C}=\text{C})$
1611	1622	$\nu(\text{C}=\text{N})$
	1595	

### FTIR and Mass Spectral measurements

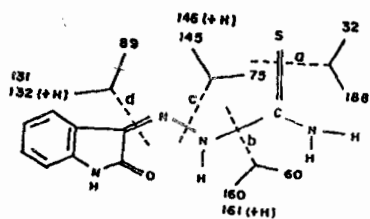
The FAB (positive) Mass Spectra were recorded on a JEOL-SZ-102 instrument having a DA-6000 data system using argon as the FAB gas in an NBA matrix. The acceleration voltage was 10kv, and the spectra were recorded at room temperature. FTIR spectra were recorded on Perkin Elmer 1800 spectrometer at Regional Sophisticated Instrumentation Centre, CDR1, Lucknow, India. Microanalysis was also done at the same centre. The E. I mass spectra were recorded on JEOL D-300/JMA - 2000, mass spectrometer/data system. The samples were introduced via a direct inlet system, ionization energy 70ev, ionization current 100 $\mu\text{A}$ , source, temperature 200 $^\circ\text{C}$ . The NICl mass spectra were recorded on a JEOL SX-102 mass spectrometer. The ion source conditions were: electron energy 200ev, emission current 100 $\mu\text{A}$ , temperature

200 $^\circ\text{C}$ . The electron capture Spectra were recorded using  $\text{CH}_4$  and a mixture of  $\text{CHCl}_3$  and  $\text{MeOH}(1:10)$  as the reagent gases.

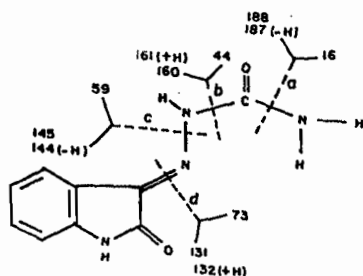
### RESULTS AND DISCUSSION

#### $^1\text{H}$ NMR Spectra

Due to the presence of  $\text{C} = \text{N}$  bond the semi-and thiosemicarbazones of isatin may have two isomeric forms as shown in Figure 1. The  $^1\text{H}$  NMR spectra of isatin-3-thiosemicarbazone and isatin-3-semicarbazone revealed only one isomeric form for each (Fig. 2 and 3, Table 1). The  $^1\text{H}$  NMR spectrum of Z-ISTSCH in  $\text{DMSO-d}_6$  exhibited eight distinct resonances (Fig. 2 Table 1). The low field singlet at 12.45ppm (exchangeable with  $\text{D}_2\text{O}$ ) was assigned to N(1)H proton (indole moiety). Expectedly, upon inspection the low field singlet at 11.20



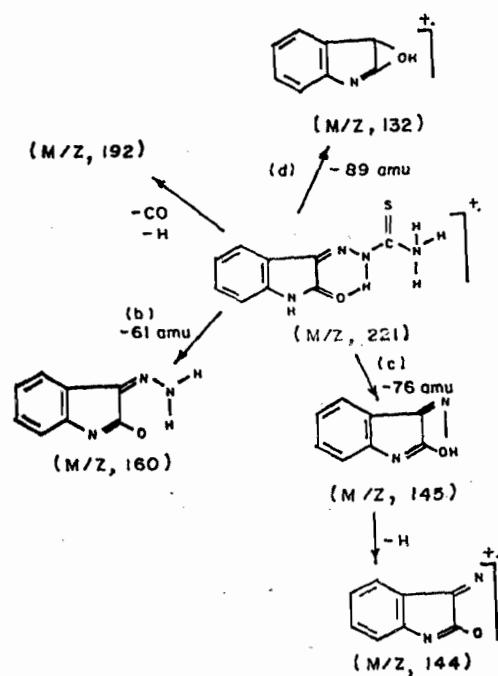
Z-ISTSCH



E-ISSCH

Scheme 1:

Primary Fragmentation of E-ISSCH and Z-ISTSCH



Scheme 2:

E.I. Fragmentation of ISTSCH.

ppm (exchangeable with  $D_2O$ ) was assigned to the N-H proton. The spectrum also exhibited two singlets (exchangeable with  $D_2O$ ) at 9.10 and 8.63 ppm assigned to the  $NH_2$  protons, suggesting hindered rotation about the C(S)- $NH_2$  bond due to its partial double bond character (Akinchan et al 1992, 1996). The four signals between 6.9 and 7.63 ppm were assigned on the basis of decoupling and NOE-difference experiments.

Table 4: Electronic spectra ( $Cm^{-1}$ ) of E-ISSCH and Z-ISTSCH in DMSO

E-ISSCH	Z-ISTSCH	Assignments
49,213	49,261	$\pi-\pi^*$ (arom)
40,984	41,254	$\pi-\pi^*$ (arom)
37,764sh	37,202sh	$\pi-\pi^*$ (C=O)
31,888	27,778	$\pi-\pi^*$ (C=N)
26,316sh	24,906sh	$n-\pi^*$ (C=N)

Table 5: E.I. and FAB (POS) mass spectra of

Isatin-3- thiosemicarbazone (ISTSCH)

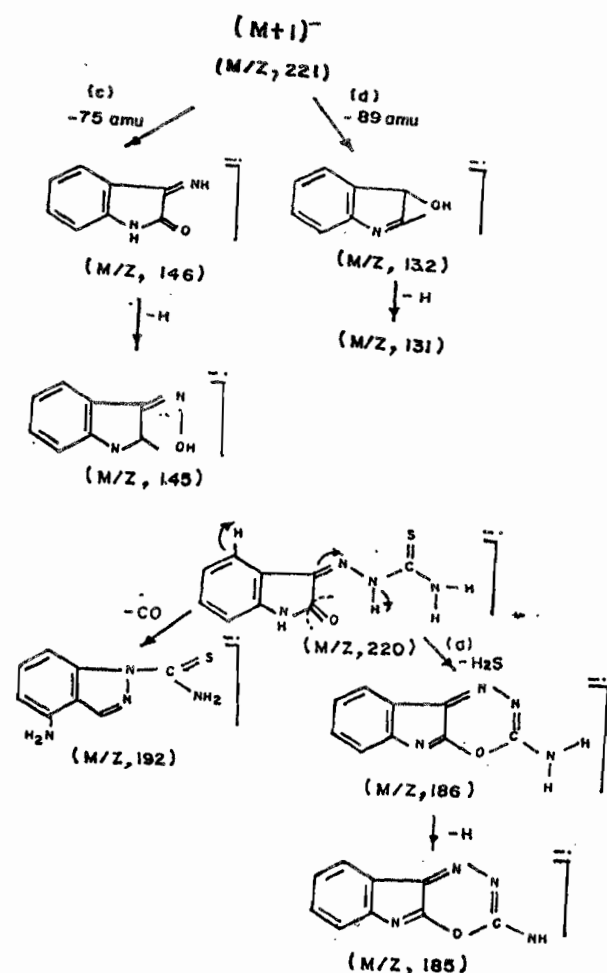
ions <sup>+</sup>	m/z	EIMS Rel. Int.	FAB (POS)MS Rel. Int.
$[M + H]^+$	221	26.10	100.00
$[M - 28]^+$	192	51.80	20.00
$[M + H - 59]^+$	162	7.30	23.17
$[M + H - 61]^+$	160	24.40	
$[M + H - 76]^+$	145	3.90	31.51
$[M + H - 77]^+$	144	9.60	-
$[M + H - 89]^+$	132	19.60	7.50
---	128	30.90	6.50
---	64	100.00	

Table 6: NICI ( $CH_4$  and  $Cl^-$ ) mass spectra of ISTSCH

Ion <sup>+</sup>	m/z	NICI( $CH_4$ ) Rel. Int.	NICI( $Cl^-$ ) Rel. Int.
$[M + ^{37}Cl]^-$	257		6.86
$[M + ^{35}Cl]^-$	255		20.91
$[M + H]^-$	221	6.60	10.09
$[M]^-$	220	45.10	
$[M - H]^-$	219	13.22	66.39
$[M - 26]^-$	194		18.85
$[M - 28]^-$	192	15.40	
$[M - 34]^-$	186	23.47	13.28
$[M - H - 34]^-$	185	10.63	100.00
$[M + H - 75 + ^{37}Cl]^-$	183		15.45
$[M + H - 75 + ^{35}Cl]^-$	181		44.59
$[M - 60]^-$	160	5.64	
$[M + H - 75]^-$	146	18.31	
$[M - 75]^-$	145	25.02	
$[M + H - 89]^-$	132	9.67	
$[M - 89]^-$	131	100.00	

Table 7: E. I. and FAB (POS) mass spectra of ISSCH

Ion <sup>+</sup>	m/z	EIMS Rel. Int.	FAB (POS) MS Rel. Int.
$[M + ^{23}Na]^+$	227		47.51
$[M + 2H]^+$	206		18.01
$[M + H]^+$	205	2.20	100.00
$[M]^+$	204	18.30	20.91
$[M + H - 17]^+$	188		47.37
$[M - 17]^+$	187	4.10	-
$[M - 28]^+$	176	1.10	18.87
$[M + 2H - 44]^+$	162	9.10	47.79
$[M + H - 44]^+$	161	100.00	32.60
$[M - 44]^+$	160	35.50	16.75
$[M - 59]^+$	145	2.90	29.30
$[M - H - 59]^+$	144	10.00	
$[M + H - 72]^+$	133	20.10	
$[M + H - 73]^+$	132	41.00	
$[M - 73]^+$	131	8.20	



Scheme 3

## Negative ion Fragmentation of ISTSCH

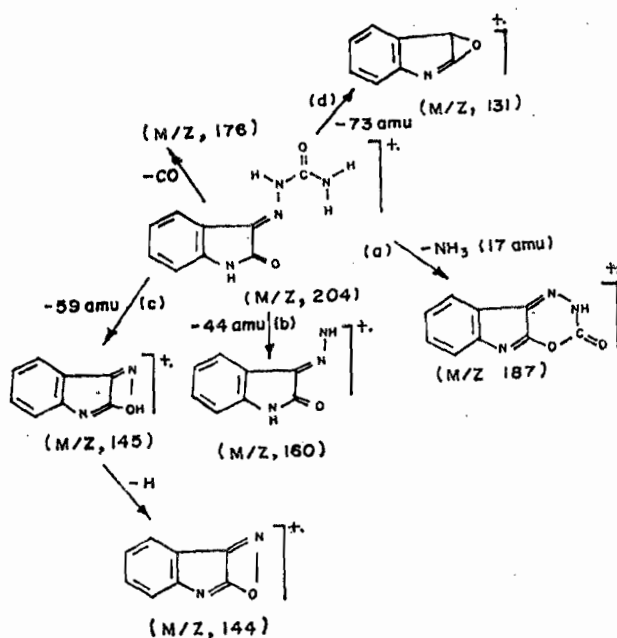
The spectrum of E-ISSCH in DMSO- $d_6$  exhibited seven distinct resonances (Table 1, Fig. 3). The low field singlet at 10.71 ppm (exchangeable with  $D_2O$ ) was assigned to N(1)H. Expectedly, upon irradiation of the N(1)H resonance a marked increase in the signal of H-4 and H-7 was observed. Enhancement of the H-4 signal is caused by NH saturation transfer. The difference between E-ISSCH and Z-ISTSCH could be identified in terms of a positive NOE on both H-4 and H-7 signals. The second low field singlet at 10.20 ppm (exchangeable with  $D_2O$ ) was assigned to the N-NH proton. The singlet at 6.91 ppm was due to  $NH_2$  protons, suggesting low energy for  $-C(O)-NH_2$  bond rotation. The large difference between E-ISSCH and Z-ISTSCH for N(1)H (indole) signal requires explanation. The relative deshielding of N(1)H in Z-ISTSCH is consistent with a withdrawal of electron density from the indole ring via  $C(2)=O$ , which is involved in intra-molecular hydrogen bonding (Fig. 2). The remaining four resonances were assigned on the basis of decoupling and NOE difference experiments.

Irradiation of the H-7 and H-4 resonances a positive NOE on H-6 and H-5 signals resulted in both E-ISSCH and Z-ISTSCH. The  $^1H$  NMR data (Table. 1) of E-ISSCH and Z-ISSCH showed a down field shift for H-4 proton in E-ISSCH (8.08ppm) compared to the signal of

Z-ISTSCH (7.63ppm) shown in Figure 2 and Figure 3.

The relative upfield shift of H-4 in Z-ISTSCH may be interpreted due to anisotropy of the  $sp^2$ -hybridized exocyclic nitrogen atom, which comes close to the H-4 in E-ISSCH (Fig. 4). In Z-ISTSCH the stereochemistry prevents such an interaction, and consequently, the H-4 is relatively more shielded (Fig. 2). In addition, the E-configuration of ISSCH was independently confirmed by  $^1H$  (NH) NOE difference experiments. Thus, for instance irradiation of the hydrazono H-NH resonance (10.20ppm) of E-ISSCH led to a marked enhancement of the H-4 proton signal (8.08ppm) (Fig. 4), whereas reverse perturbation of the latter resonance strongly affected the hydrazone, N-NH signal to much greater extent, besides the N(1)H (NH-exchange) and H-5 signals (Fig. 5). This through-space connection between NH proton and the H-4 proton is only possible in the E-configuration of ISSCH (Heinisch and Holzer, 1990, Easmon et al. 1993). Further, more irradiation of the N(1)H resonance (10.71ppm) of E-ISSCH leads to a marked enhancement of the doublet at 6.88ppm (H-7) to greater extent, whereas reverse perturbation of the later resonance strongly affected the N(1)H and the H-6 signal.

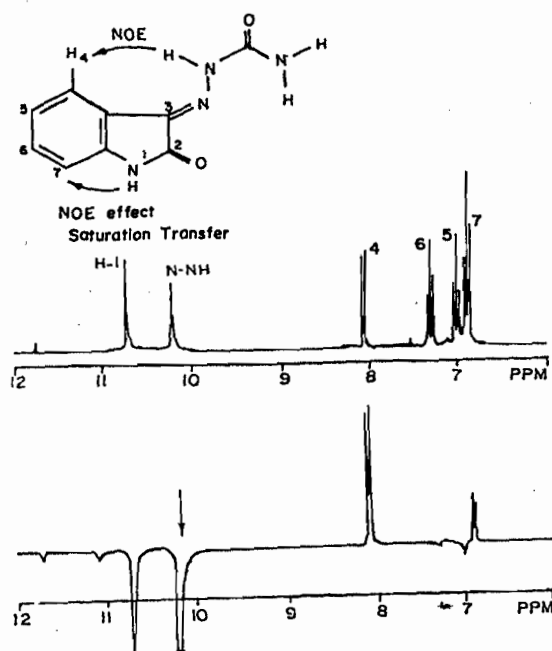
The NOE-difference experiments with Z-ISTSCH were done and the following observations were made. Irradiation of the N(1)H resonance (12.45ppm) led to a marked enhancement of the doublet at 6.90 ppm (H-7) (Fig. 6). On the otherhand, no NOE was observed on the NH signals when irradiating the H-4 resonance. Thus, the Z-configuration has to be assigned to ISTSCH (Heinisch and Holzer 1990, Eashon et al. 1993). Furthermore, irradiation of the  $NH_2$  signal at 9.01ppm enhanced H-7(Fig.7), but irradiation at 8.63ppm enhanced both H-4 and H-7 signals in Z-ISTSCH.



Scheme 4.

## E. I. Fragmentation of ISSCH.





(a)  $^1\text{H}$  NMR spectrum of E-ISSCH in  $\text{DMSO}-d_6$ .

Figure 4:

(b) NOE difference spectrum of E-ISSCH resulting from irradiation of N-NH proton signal at 10.20ppm.

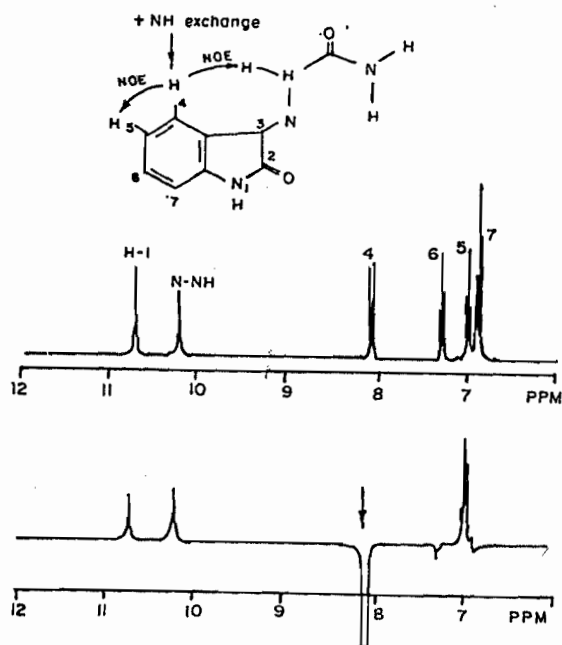


Figure 5:

(a)  $^1\text{H}$  NMR spectrum of E-ISSCH in  $\text{DMSO}-d_6$

(b) NOE difference spectrum of E-ISSCH resulting from irradiation of H-4 proton signal at 8.08ppm

assignment described above. In Z-ISTSCH, the N-NH and H-4 are trans to each other, and the  $\gamma$ -effect is not observed.

### IR Spectra

The characteristic spectral bands in the IR spectra of E-ISSCH and Z-ISTSCH are summarized in Table 3. The absence of  $\nu(\text{SH})$  absorption in the region  $2500\text{--}2600\text{cm}^{-1}$  for Z-ISTSCH clearly suggests the thione tautomeric form (Akinchan et al. 1992). The  $\nu(\text{C}=\text{O})$  stretching frequency (indole moiety) is of low energy in Z-ISSCH ( $1700\text{ cm}^{-1}$ ) compared to E-ISSCH ( $1725\text{ cm}^{-1}$ ), which supports the intramolecular hydrogen bonding (Fig. 2). The  $\nu_{\text{as}}(\text{NH}_2)$  and  $\nu_{\text{s}}(\text{NH}_2)$  were observed at  $3520$  and  $3424\text{ cm}^{-1}$  respectively, in the spectrum of Z-ISTSCH. The E-ISSCH's spectrum shows these bands at  $3464$  and  $3412\text{ cm}^{-1}$  respectively. The higher energy for  $\nu_{\text{as}}(\text{NH}_2)$  in Z-ISTSCH could be attributed to increased asymmetry to  $\text{NH}_2$  group. This is further supported by the higher energy for  $\delta(\text{NH}_2)$  in Z-ISTSCH's spectrum. The asymmetric  $\nu_{\text{as}}(\text{NH}_2)$  stretch is being strongly affected and is of lower energy in E-ISSCH due to intramolecular hydrogen bonding involving iminyl nitrogen ( $\text{C}=\text{N}$ ) and  $\text{NH}_2$  group hydrogen ( $\text{C}=\text{N} \dots \text{H}-\text{NH}$ ). Furthermore,  $\nu(\text{NH})$  stretching frequency is lowered in Z-ISTSCH ( $3170\text{ cm}^{-1}$ ) compared to E-ISSCH ( $3238\text{ cm}^{-1}$ ) supports intramolecular hydrogen bonding involving  $\text{C}=\text{O}$  (indole moiety) and hydrogen of (N-NH) as shown in Figure 2.

### Electronic Spectra

The electronic spectra of E-ISSCH and Z-ISTSCH taken in dimethyl sulphoxide solution are reported in Table 4. The electronic bands above  $38,000\text{ cm}^{-1}$  are assigned to  $\pi \rightarrow \pi^*$  electronic transition of aromatic system (Akinchan et al 1996). The spectrum of Z-ISTSCH shows  $\pi \rightarrow \pi^*$  transition at  $27,778\text{ cm}^{-1}$  involving iminyl nitrogen ( $\text{C}=\text{N}$ ) of thiosemicarbazone moiety. The E-ISSCH's spectrum shows this electronic transition at higher energy ( $31,888\text{ cm}^{-1}$ ) probably due to E-conformation. Below  $30,000\text{ cm}^{-1}$  most of the thiosemicarbazone shows electronic band due to  $n \rightarrow \pi^*$  electronic transition associated with thiosemicarbazone moiety. The energy of the transition depends on the isomeric form of the thiosemicarbazone and involvement of N-NH in hydrogen bonding. Thus, the Z-conformation for ISTSCH is suggested.

Table 8:  $\text{NiCl}(\text{CH}_4 \text{ and } \text{Cl}^-)$  mass spectra of ISSCH

ION*	m/z	$\text{NiCl}(\text{CH}_4)$ Rel. Int.	$\text{NiCl}(\text{Cl}^-)$ Rel. Int.
$[\text{M} + ^{37}\text{Cl}]$	241	---	17.87
$[\text{M} + ^{35}\text{Cl}]$	239	---	55.85
$[\text{M} + \text{H}]$	205	13.45	---
$[\text{M}]^-$	204	100.00	13.00
$[\text{M} - \text{H}]^-$	203	8.58	100.00
$[\text{M} + \text{H} - 44]$	161	16.28	---
$[\text{M} + \text{H} - 59]$	146	6.60	---
$[\text{M} + \text{H} - 73]$	132	6.56	---
$[\text{M} - 73]$	131	62.02	---

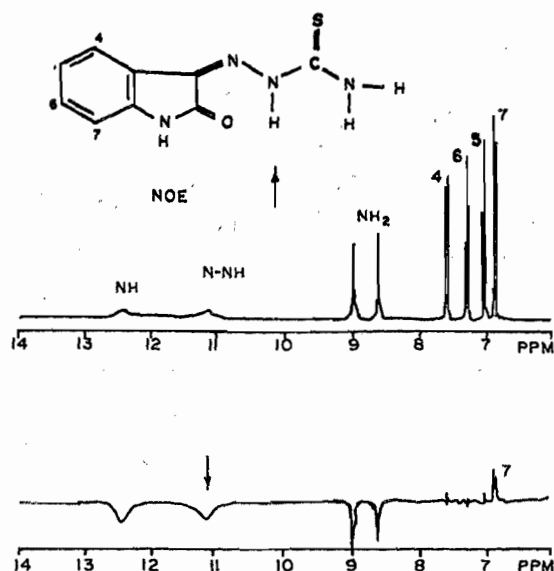


Figure 6:

- (a)  $^1\text{H}$  NMR spectrum of Z-ISTSCH in  $\text{DMSO}-d_6$ .  
 (b) NOE-difference spectrum of Z-ISTSCH resulting from irradiation of N-NH proton signal at 11.12ppm.

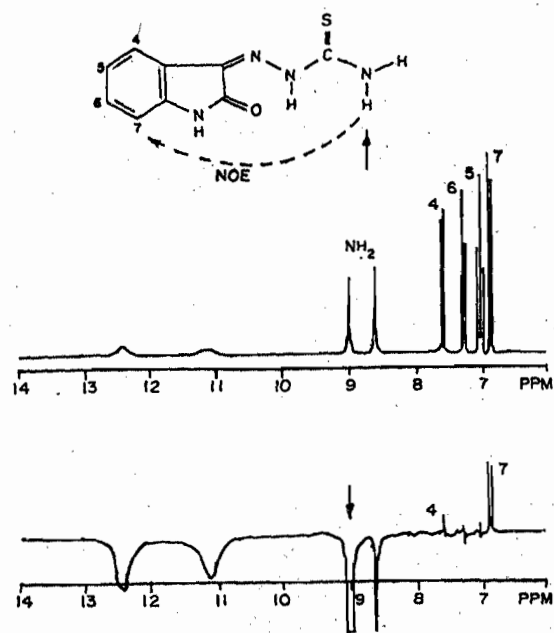
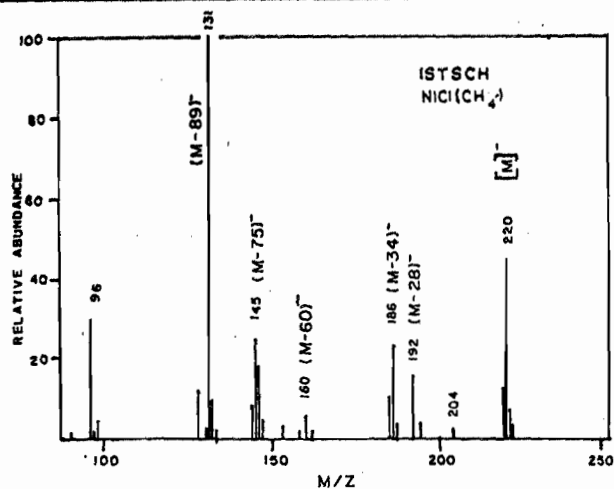


Figure 7:

- (a)  $^1\text{H}$  NMR spectrum of Z-ISTSCH in  $\text{DMSO}-d_6$ .  
 (b) NOE difference spectrum of Z-ISTSCH resulting from irradiation of  $\text{H}_2$  proton signal at 9.01ppm.

### Isatin-3-Thiosemicarbazone: E.I. and FAB Mass Spectra.

Table 5 shows the partial E. I. and FAB (POS) mass spectra of ISTSCH. Scheme 1 summarises the

Figure 8:  $\text{NICl}(\text{CH}_4)$  mass spectrum of ISTSCH

primary fragmentation pattern. Only molecular ion and the structurally most important fragments are presented. The molecular ion peak is absent but  $[\text{M} + \text{H}]^+$  is observed both in E. I. and FAB (POS) spectra. The FAB spectra is more useful for the molecular weight estimation. The essential feature of the FAB spectrum of ISTSCH is the presence of protonated molecular ion as a base peak. The E. I. spectrum shows base peak at  $m/z$ , 64. It has been reported that isatin loses CO, HCN and CO successively from the molecular ion during mass spectral fragmentation. In the present case Isatin-3-thiosemicarbazone gave  $m/z$  192 as a fragmentation product due to loss of one CO group. The other most abundant ions are located at  $m/z$ , 162, 160, 145, 144, and 132. The mass losses observed may be rationalized as shown in Scheme 2.

### Isatin-3-Thiosemicarbazone: Negative Ion Chemical Ionization Mass Spectra.

Figure 8 and Table 6 show the ion abundances in the  $\text{NICl}(\text{CH}_4)$  spectra of ISTSCH. The presence of  $\text{C}=\text{O}$ ,  $\text{C}=\text{N}$  and  $\text{C}=\text{S}$  having  $\pi$ -anti bonding molecular orbitals are the possible sites to accommodate the captured electron. The  $[\text{M} + \text{H}]^+$ ,  $[\text{M}]^+$  and  $[\text{M}-\text{H}]^+$  are observed in  $\text{NICl}(\text{CH}_4)$  spectrum with  $[\text{M}]^+$  at  $m/z$ , 220 of highest intensity (45.10%). The  $[\text{M}]^+$  ion is not observed in  $\text{NICl}(\text{Cl}^-)$  spectrum. The  $[\text{M}-\text{H}]^+$  at  $m/z$  219 is the most abundant in  $\text{NICl}(\text{Cl}^-)$  spectrum indicating loss of proton from the molecule of ISTSCH and one molecule of HCl had been eliminated. The pseudo molecular ion  $[\text{M}-\text{H}]^+$  is stable due to hydrogen bonding  $\text{C}=\text{O} \cdots \text{HN}$  as shown in Scheme 3. This ion further fragments to produce  $m/z$  185 (100%) via  $m/z$ , 186 by the loss of HS and H successively (Scheme 3). The base peak in  $\text{NICl}(\text{CH}_4)$  spectrum has been observed at  $m/z$ , 131. Here electron capture occurs at  $\text{C}=\text{N}$  anti bonding  $\pi$ -orbital and the  $^3\text{C}-\text{N}$ -bond is being cleaved. The ion peaks at  $m/z$ , 257 and 255 with a characteristic chlorine isotopic pattern (1:3 ratio) also supports the existence of molecular ion. These ion peaks fragment to  $m/z$ , 183 and  $m/z$  181 having characteristic chlorine isotopic pattern (Table 6). The formation of other ion peaks and the mass losses could be rationalized as shown in Scheme 3.

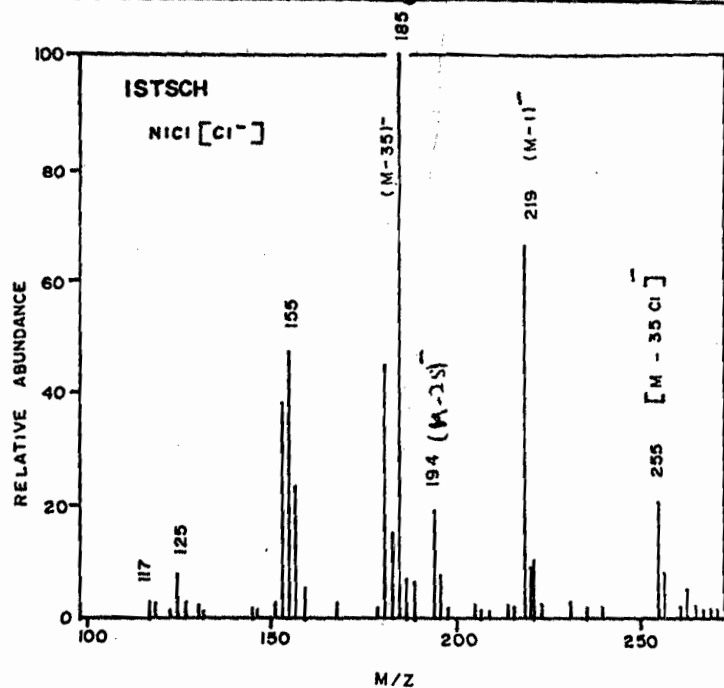
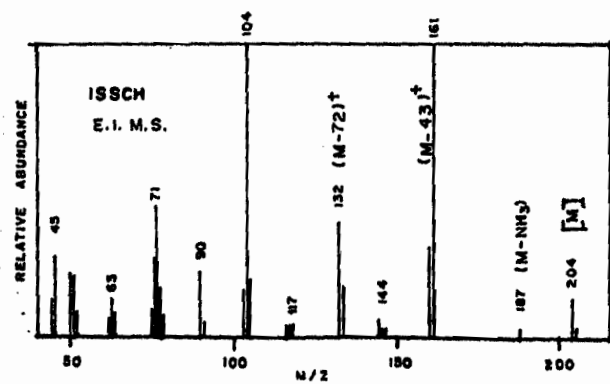
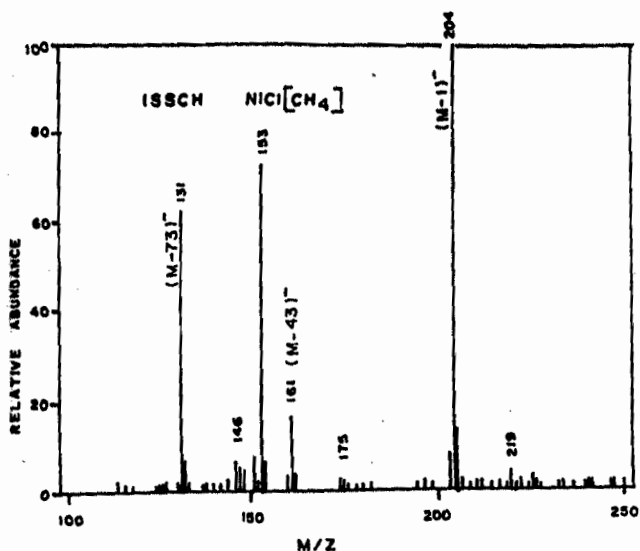
Figure 9:  $\text{N1Cl}(\text{Cl}^-)$  mass spectrum of ISTSCH

Figure 10. E. I. mass spectrum of ISSCH

Figure 11:  $\text{N1Cl}(\text{CH}_4)$  mass spectrum of ISSCH.

#### Isatin-3-Semicarbazone: E. I. and FAB Mass Spectra

Figure 10, and Table 7 exhibit the EI and FAB(POS) mass spectra of ISSCH. The molecular ion peak is present in both spectra having lower abundance profile. The FAB(POS) spectrum exhibits  $[\text{M} + \text{H}]^+$  at  $m/z$  205 as a base peak. The ion peak at  $m/z$ , 227  $[\text{M} + {}^{23}\text{Na}]^+$  formed by cationization of molecular ion has also been observed. It is formed probably due to sodium salt contamination during preparation of ISSCH (Biswas et al. 1978). The presence of this in the spectrum is able to distinguish between  $[\text{M}]^+$   $[\text{M} + \text{H}]^+$  ions. The presence of protonated molecule as a base peak is useful for the unambiguous estimation of molecular weight. The E. I. mass spectrum exhibits base peak at  $m/z$ , 161, due to easier cleavage of  $\text{H}^2\text{N} - \text{C}(\text{O})$  bond. The similar observation have been reported for the mass spectral fragmentation of 3-Isatin benzoyl hydrazone (Verma and Pandey, 1983). The mass losses observed during formation of most abundant ions may be rationalized as shown in Scheme 4.

#### Isatin-3-Semicarbazone: Negative Ion Chemical Ionization Mass Spectra.

Table 8 records the ion abundance in the  $\text{N1Cl}(\text{CH}_4)$  and  $\text{N1Cl}(\text{Cl}^-)$  spectra of ISSCH. The presence of  $\text{C} = \text{O}$ ,  $\text{C} = \text{N}$  having  $\pi$ -anti bonding molecular orbitals are able to accommodate the captured electron. The  $[\text{M}]^-$  at  $m/z$  204 in  $\text{N1Cl}(\text{CH}_4)$  and  $[\text{M} - \text{H}]^-$  at  $m/z$ , 203 in  $\text{N1Cl}(\text{Cl}^-)$  are the base peaks in the spectra of ISSCH. The  $\text{Cl}^-$  ion being more basic could easily deprotonate the molecular ion to produce  $\text{HCl}$  and the stable  $[\text{M} - \text{H}]^-$  ion. The existence of a molecular ion is also exhibited by the presence of ions at  $M/z$ , 241  $[\text{M} + {}^{37}\text{Cl}]^-$  and  $m/z$ , 239  $[\text{M} + {}^{35}\text{Cl}]^-$  with a characteristics chlorine isotopic pattern.



## CONCLUSION

Based on  $^1\text{H}$  NMR spectroscopy, including NOE difference experiments, the configuration of ISTSCH and ISSCH could be determined unequivocally. The ISTSCH exists mainly in the Z-form and the ISSCH turned out to be E-isomer in DMSO solution. The  $^{13}\text{C}$  NMR spectra support the results obtained from the  $^1\text{H}$  NMR spectral study. Further support came from the IR spectral measurement in the solid state. The mass spectral data also support the proposed configuration for the compounds under investigation.

## ACKNOWLEDGEMENT

The author is grateful to Professor G. Heinisch, of the University of Innsbruck and Professor W. Holzer of the University of Vienna, both in Austria and Professor M. Graziani of the University of Trieste, Italy for providing NMR spectral data. Thanks are also due to Heads of the Regional Sophisticated Instrumentation Centres at the CDRI, Lucknow and IIT, Chennai, India for technical assistance in obtaining micro analysis, electronic, FTIR,  $^1\text{H}$  and  $^{13}\text{C}$  NMR and FAB (positive), NICI ( $\text{CH}_4$ ) and NICI ( $\text{Cl}^-$ ) mass spectra.

## REFERENCES

- Akinchan, N. T.; Akinchan, R. and Drozdowski, P. M., 1996. Nuclear Magnetic Resonance and vibrational spectral studies on Platinum (II) complexes of thiosemicarbazone derived from fluorenone; Polish J. Chem. 70: 171 – 179.
- Akinchan, N. T. Akinchan, R; Ibok, U. J; Battaglia, L. P., Corradi, A. B., and Drozdowski, P., 1992. Synthesis, spectroscopic characterization of thiosemicarbazone complexes of Nickel (II) and x-ray structures of anisaldehyde thiosemicarbazone; and bis (tolualdehyde thiosemicarbazone) nickel (II), Cryst. Spectr. Research, 22(6): 741-753.
- Akinchan, N. T., Akinchan, R., West, D. X. and Yang, Y. H., 1994. Magnetic measurements and spectral studies on Copper (II) complexes of semicarbazones derived from isatin, benzoin and 2-hydroxy-1-naphthaldehyde. Transition Met. Chem. 19: 135 – 140.
- Akinchan, N. T.; Drozdowski, P. M. and Holzer, W., 2002. Syntheses and spectroscopic studies on Zinc(II) and Mercury (II) complexes of isatin-3-Thiosemicarbazone, J. Mol. Structure, 641: 17 - 22.
- Angell, E. C. Black, D. St.C. and Kumar, N. 1992.  $^{13}\text{C}$  NMR study of N-acyl-and N-Sulphonyl-isatins and their Ring opened Derivatives; Magn. Reson. Chem. 30: 1 – 5.
- Bişwas, K. M., Ali, M. E.; Jackson, A. H. and Games, D. E., 1978. Application of Field Desorption and Electron Impact spectrometry and NMR spectroscopy in the study of Flavonoid-o-Glycosides; J. Indian Chem. Soc. 55: 1240 – 1245.
- Chatterjee, P., Agarwala, B. V., Dey, A. K., 1989. New octahedral complexes of Schiff Bases derived from 2,3 – Indolinedione; Synth. React. Inorg. Met-org. chem. 19(7): 715-730.
- Easmon, J. ; Heinisch, G. and Holzer, W. 1993. On the stereochemistry of Novel Biologically Active Diazine-Derived Thiosemicarbazones; Sci. Pharm. 61: 3 – 10.
- Heinisch, G. and Holzer, W., 1990. On the Application of Homonuclear NOE Difference spectroscopy as a convenient tool for configurational Assignments of compounds with C=N bond, Monatsh. Chemie, 121: 837 – 846.
- Ivanov, V. E., Tikhomirova, N. G. and Tom Chin, A. B., 1988. Copper (II) and Copper (I) complexes with Isatin-3-Thiosemicarbazones Zh. Obshch. Khim; 58(12): 2737 – 2743.
- Labisbal, E.; Sousa-Pedrares, A; Kaminsky, W. and West, D. X., 2002. Structures of N-methyl isatin N(4) – Dimethyl Thiosemicarbazone and its Electrochemically synthesized 6-coordinate Cadmium (II) complex., Z. Naturforsch, 57b: 908 – 913.
- Levinson, W. E., 1980. Chelating substances; Antibiotics Chemother. 27: 288 - 306.
- Levy, J. A., Levy, S. B. and Levinson, W., 1976. Inactivation of Murine RNA tumour viruses by Isatin-beta-Thiosemicarbazone, its Derivatives and Analogs, Virology, 74(2): 426 – 431.
- Selem, H. S. M., El-Behairy, M; Mashaly, M. M. and Mena, H. H., 2002. Thermodynamics of complexation of Isatin-3-Thiosemicarbazone and other related derivatives with some Metal ions, J. Serb. Chem. Soc. 67(4): 243 – 256.
- Sherman, L., Edelstein, F., Shtacher, G., Avramoff, M., and Teitz, Y., 1980. Inhibition of Moloney Leukaemia virus production by N-methyl- Isatin-beta-4,4-diethyl thiosemicarbazone; J. Gen. Virology, 46(1): 195 – 203.
- Verma, R. S. and Pandey, K. 1983. Mass spectral studies of 3-(p - fluoro) benzoylhydrazone-2-indolinones, J. Indian Chem. Soc. 60: 272 – 274.
- Wang, L. H. and Levinson, W., 1978. N-methyl isatin-beta-thiosemicarbazone Copper (II) complex inhibits RNA-dependent DNA polymerase but not Ribonuclease H of Rous Sarcoma virus. Bjo-Inorg. Chem. 8(6): 535 – 540.
- West, D. X.; El-Sawaf, A. K. Bain, G. A., 1998. Spectral study on N-methyl isatin N(4)-dimethyl thiosemicarbazone and its Cobalt(II), Nickel(II) and Copper(II) complexes; Transition Met. Chem. 23: 1 – 3